A calculation of the temperature-dependent susceptibility of Pd and dilute $Pd_{1-x}Ag_x$ and PdH_x alloys

1994 J. Phys.: Condens. Matter 6 2603

(http://iopscience.iop.org/0953-8984/6/13/018)

J. Phys.: Condens. Matter 6 (1994) 2603–2618. Printed in the UK

A calculation of the temperature-dependent susceptibility of Pd and dilute $Pd_{1-x}Ag_x$ and PdH_x alloys

B Kirchner, W Weber and J Voitländer

Institut für Physikalische Chemie, Universität München, Sophienstrasse 11, 80333 München, Germany

Received 2 November 1993, in final form 14 December 1993

Abstract. The temperature dependence of the magnetic properties of itinerant electron systems is mainly due to the excitation of spin fluctuations. We calculate the susceptibilities of Pd, $Pd_{1-x}Ag_x$, and PdH_x ($0 \leqslant x \leqslant 0.03$) with an extension of the classical Murata–Doniach model for spin fluctuations, which treats the energy functional without a Landau expansion of the magnetization-dependent ground state energy. To obtain this energy ASW (augmented spherical wave) and KKR–CPA bandstructure calculations are performed. In agreement with experiment the KKR–CPA method yields a maximum of $\chi(T)$ for Pd, which disappears with increasing Ag concentration. In the ASW calculations, low Ag and H concentrations are simulated by the supercells $Pd_{31}Ag$ and $Pd_{32}H$. In addition the alloy PdH_x is simulated by calculations for pure Pd, with the valence electron concentration increased suitably.

Calculations of the susceptibility of Pd within the framework of the Stoner theory and the spin fluctuation theory based upon the rigid-band model are presented. The role of the electron interaction in both theories is examined and the reason for the maximum of $\chi(T)$ for Pd is investigated. We find the different scaling of the temperature axis in the Stoner and spin fluctuation theories to have its origin in a different treatment of the electron interaction.

1. Introduction

The temperature-dependent susceptibility of Pd and Pd-rich intermetallic compounds has been measured by several authors [1, 2, 3, 4] since the 1960s. It is a remarkable fact that the magnetic susceptibility of pure Pd shows a maximum at about 80 K. Early theoretical investigations within the frame of the Stoner theory by Shimizu *et al* [5] and Hahn and Treutmann [3] related this effect to a positive curvature of the density of states of Pd at the Fermi level. Theoretical improvements were made by Liu *et al* [6] who treated the electron exchange–correlation interaction self-consistently at finite temperature within the variational approach of Vosko and Perdew [7]. Irkhin and Rosenfeld [8] assumed a discontinuity of the derivative of the density of states near the Fermi level from which they could explain the temperature-dependent susceptibility of Pd on the basis of Stoner's theory.

Nevertheless, extensive investigations on weak itinerant ferromagnets and nearly ferromagnetic metals revealed spin fluctuations to be the most important excitations in the low-temperature regime; these are totally neglected in Stoner's theory. Thus, the discussion of thermal properties of these materials should be in terms of spin fluctuation theory. Mohn and Schwarz [9] performed spin polarized bandstructure calculations for Pd, to obtain the total energy for a set of magnetizations. A Ginzburg–Landau polynomial fit of these data was taken as input for the Murata–Doniach model [10] for spin fluctuations. The susceptibility curve obtained in this way also exhibits a maximum.

0953-8984/94/132603+16$19.50

In a recent paper [11] we introduced a new method for the calculation of the temperature-dependent spin susceptibility of weakly correlated itinerant metals. We generalized the classical treatment of magnetization fluctuations first proposed by Murata and Doniach. Our generalization went beyond the Ginzburg–Landau expansion of the energy functional. In this paper we present results for the temperature-dependent susceptibility of Pd and of the alloys $Pd_{1-x}Ag_x$ and PdH_x in the concentration range $0 \leqslant x \leqslant 0.03$. The required bandstructure calculations were carried out self-consistently employing the ASW [12] and KKR–CPA [13, 14] methods.

Finally, we apply Stoner's theory to compare the susceptibility curves based upon single-particle excitations with those obtained in the framework of spin fluctuation theory.

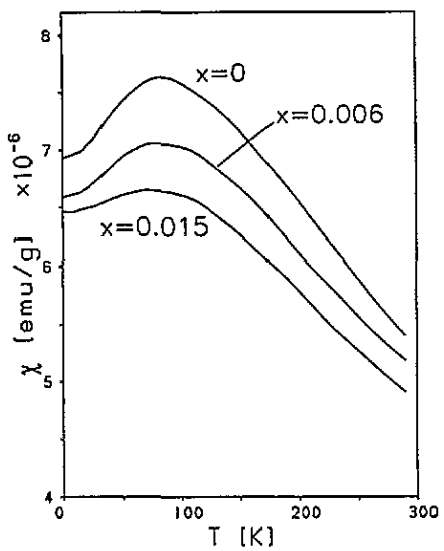

Figure 1. The measured susceptibility of $Pd_{1-x}Ag_x$ versus temperature [15].

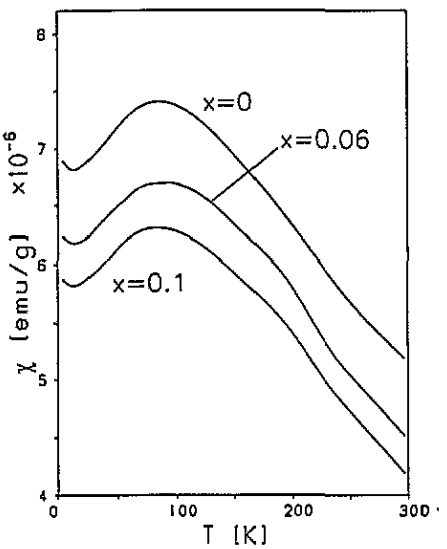

Figure 2. The measured susceptibility of PdH_x versus temperature [4].

The experimental results for the susceptibility of the $Pd_{1-x}Ag_x$ and PdH_x alloys are shown in figures 1 and 2, respectively. In silver alloys the absolute values of the susceptibility decrease and the maximum vanishes at about 3% Ag. In the PdH_x alloys a similar decrease of the susceptibility with growing hydrogen concentration was observed by Jamieson and Manchester [4], yet the whole curve is scaled to smaller values while its shape remains unchanged for concentrations below 40% H. The authors ascribed this effect to the coexistence of two hydrogen phases in the Pd host, where the α-phase exists alone for H concentrations below 3%.

The susceptibility maximum of Pd and its dependence on the concentration of impurities provides a critical test for our method.

2. Outline of the theory

In former papers [16, 9] the energy functional was written in the form of a Landau polynomial

$$\mathcal{H} = \int \left[\frac{A}{2} m^2(r) + \frac{B}{4} m^4(r) + \frac{C}{6} m^6(r) + \frac{D}{2} \sum_i [\nabla m_i(r)]^2 \right] \mathrm{d}^3 r$$

where the coefficients A, B and C were determined by a fit of the magnetization-dependent energy curve obtained by spin polarized bandstructure calculations. As already mentioned in [11] these coefficients depend strongly on the magnetization range of the fit. Alternatively the same coefficients may be obtained by fitting a polynomial to the curve $B(M) = E'(M)$, where B is the external field that stabilizes the magnetization M. Since changes in M produce insignificant changes in E with bad consequences on the numerical accuracy, it is favourable to use the $B(M)$ curve, which may also directly be extracted from a bandstructure program. Nevertheless, in both procedures the results for the coefficients of the fit are strongly affected by the M-range of the fit. To demonstrate this we carried out spin polarized ASW bandstructure calculations for Pd to obtain the $E(M)$ and $B(M)$ curves. A least-squares fit of these curves of orders six and five in the range $M \in [0, M_{\max}]$ was used to calculate the coefficients A, B and C introduced above. Figures 3 and 4 show the coefficients versus $M_{\max}$ for both methods. The strong dependence on $M_{\max}$ is remarkable.

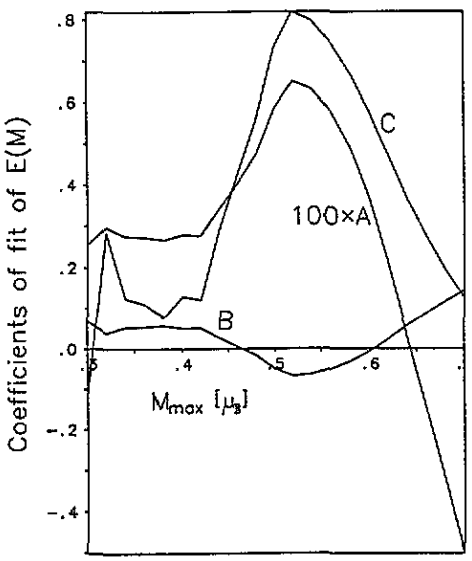

Figure 3. Coefficients A, B and C (in Ryd$\times\mu_B^{-n}$ with $n = 2, 4, 6$) of the $E(M)$ curve of Pd as a function of the upper boundary of the fit. The bandstructure calculations were carried out with the ASW method. Lattice parameter 7.4 au.

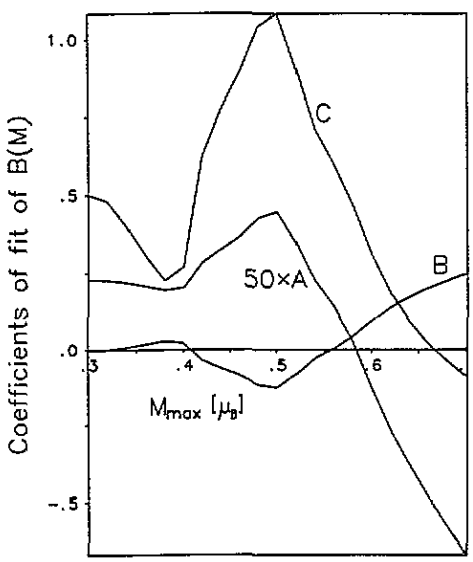

Figure 4. Corresponding coefficients for $B(M)$ (all else as in figure 3).

With our new method, which does not fit a polynomial to the $E(M)$ or $B(M)$ data, we could derive the following formula for the temperature-dependent inverse susceptibility:

$$\chi^{-1}(\langle m^2\rangle) = \frac{\sqrt{2/\pi}}{\langle m^2\rangle^{3/2}} \int_0^\infty \left[\frac{E''(M)}{3} + \frac{2E'(M)}{3M}\right] M^2 \exp\left(-\frac{M^2}{2\langle m^2\rangle}\right) \mathrm{d}M. \quad (1)$$

Here the mean square of the fluctuations is given by

$$\langle m^2\rangle = \frac{k_B T}{2\pi^2} \int_0^{q_c} \frac{q^2}{\chi^{-1}(\langle m^2\rangle) + \chi^{-1}(q) - \chi^{-1}(0)} \mathrm{d}q \quad (2)$$

where $\chi(q)$ is the wavevector-dependent susceptibility for $T = 0$. Equations (1) and (2) implicitly determine the form of $\chi(T)$. The cut-off wavevector q_c sets a limit for the number of classical fluctuation modes contributing to the free energy of the system. A temperature dependence of the cut-off wavevector like $q_c \sim T^{1/3}$ has already been proposed by Murata [17] and Lonzarich and Taillefer [18]. In [19] we presented a microscopic foundation of the Murata–Doniach model and its energy functional. We derived an explicit formula for $q_c(T)$

$$q_c = q_0 T^{1/3}. \quad (3)$$

q_0 was estimated as

$$q_0 = \left(\frac{4\pi^2\gamma}{V_{mol} k_B}\right)^{1/3} \quad (4)$$

with V_{mol} being the volume per mole, and γ the coefficient of the molar electronic heat capacity.

Equations (2) and (3) lead to a quadratic increase of $\langle m^2\rangle$ with T at low temperatures, and to a linear increase at higher temperatures (see figure 5). Since the term

$$\frac{E''(M)}{3} + \frac{2E'(M)}{3M}$$

in (1) is the mean of longitudinal and transverse inverse susceptibility, and

$$\frac{\sqrt{2/\pi}}{\langle m^2\rangle^{3/2}} M^2 \exp\left(-\frac{M^2}{2\langle m^2\rangle}\right)$$

is the Maxwellian distribution function with the maximum at $M = \sqrt{2\langle m^2\rangle}$, equation (1) represents an average of the inverse susceptibility over spatial components and magnetization. As can be seen from figure 5 the $\langle m^2\rangle$-value corresponding to $T = 100$ K is $10^{-3}\mu_B{}^2$. Thus, for temperatures below 100 K, the Maxwellian has a very sharp peak at M-values below $0.05\mu_B$ and the investigation of the susceptibility in the range 0–100 K requires a very accurate calculation of the integrand in this low-M regime.

When χ is calculated for an arbitrary temperature in terms of a Landau expansion, the $B'(M)$ curve as a whole enters the theory through the expansion coefficients, whereas our new method just makes use of that part of $B'(M)$ met by the fluctuations.

3. ASW results

We have calculated the electronic structure of the FCC Pd host using the fixed spin moment method (FSM) [20] for a set of 51 M-values in the range of 0–$0.56\mu_B$ with an increment

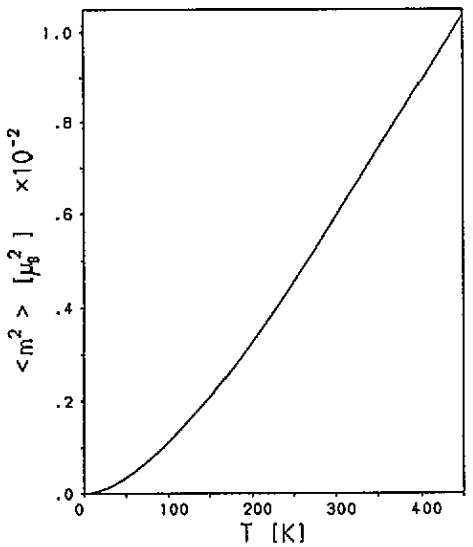

Figure 5. The dependence of $\langle m^2 \rangle$ on T for an ASW calculation of the susceptibility of Pd; lattice parameter 7.425 au.

of $0.005\mu_B$ for small M-values. From the difference of the Fermi energies for spin up and spin down we obtain the magnetic field corresponding to each M-value as

$$B(M) = \frac{\epsilon_F^{\uparrow} - \epsilon_F^{\downarrow}}{2\mu_B}.$$

We fit a cubic spline to these data points and perform the differentiation of B and the subsequent integration in equation (1) analytically. We then evaluate equation (1) only for such values of $\langle m^2 \rangle$ for which the error due to finite integration is smaller than one per cent. This sets an upper boundary for the temperatures with reliable results for χ. In order to evaluate (2), data for the wavevector-dependent susceptibility at 0 K were taken from *ab initio* calculations on Pd performed by Stenzel and Winter [21], and were fitted to the parametrization

$$\chi^{-1}(q) = \chi^{-1}(0)(1 + \sigma^2 q^2).$$

The integration in (2) can then be performed analytically. q_0 was chosen to achieve the best possible correspondence between theoretical and experimental curves at high temperatures. This procedure of fixing q_0 was applied to all susceptibility curves throughout this paper. The values for q_0 found in this way are close to that estimated from equation (4). A numerical inversion of equation (2) yielded $T(\langle m^2 \rangle)$.

The curves for the lattice parameters 7.333, 7.4 and 7.425 au shown in figure 6 were obtained from a non-relativistic calculation with 770 k-vectors in the irreducible wedge of the first Brillouin zone. For all three curves the susceptibility maximum is reproduced. The experimental curve for pure Pd in this and all following figures was generated from data of Jamieson and Manchester [4] (below 300 K) and Weiss and Kohlhaas [2] (300–800 K). The best agreement with experiment is achieved with the equilibrium lattice parameter $a = 7.425$ au, whereas the experimental lattice parameter 7.333 au corresponds to the lowest curve.

Calculations with a scalar relativistic version of the ASW program at best yielded a poor maximum at too low temperature.

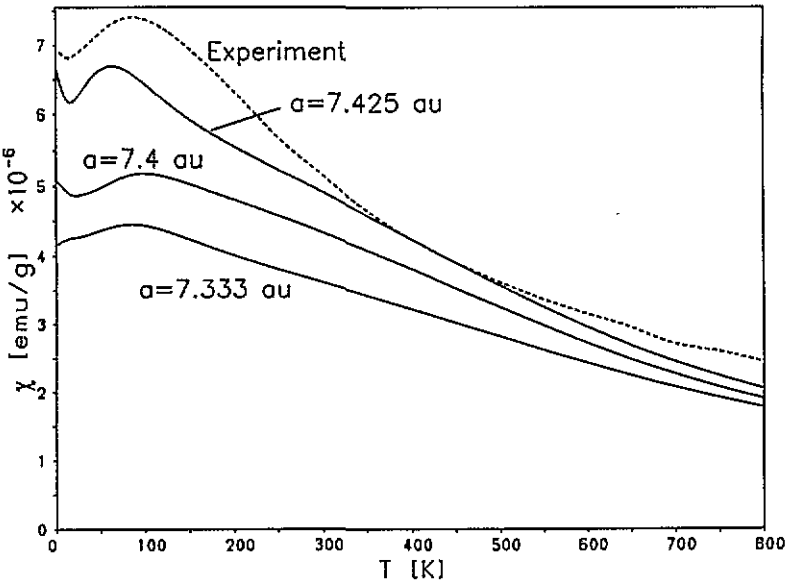

Figure 6. The susceptibility of Pd based on non-relativistic ASW calculations for lattice parameters 7.333, 7.4 and 7.425 au. The corresponding values of q_0 are 0.06, 0.056 and $0.05 \times 2\pi a^{-1}$ K$^{-1/3}$.

To simulate the susceptibility of the alloy systems $Pd_{1-x}Ag_x$ and PdH_x in the low concentration regime, ASW calculations for $Pd_{31}Ag$ and $Pd_{32}H$ supercells of simple cubic structure were performed.

The hydrogen in PdH fills octahedral interstices while PdAg is a substitutional alloy. The different shells of the palladium atoms for both supercells and the corresponding number of symmetry-equivalent atoms of the basis are given in table 1. To keep the amount of computer time within reasonable limits, we had to restrict the number of k-vectors in the irreducible wedge to 20 during integration over the Brillouin zone. The geometry of the supercell $Pd_{31}Ag$ and the atoms of the basis are sketched in figure 7.

Table 1. The numbers of equivalent atoms in different shells of the $Pd_{31}Ag$ and $Pd_{32}H$ supercells.

	Equivalent atoms	
Shell	$Pd_{31}Ag$	$Pd_{32}H$
1	12	6
2	3	8
3	12	12
4	3	6
5	1	—

In order to compare our results from these supercell calculations with those for pure Pd we had to choose the same k-vectors for the Brillouin zone integration. We therefore used a Pd_4 supercell with 120 k-points, which matches the k-mesh of the Pd_{32} cell. Figure 8 shows the susceptibility curve for $Pd_{31}Ag$ and the corresponding Pd_4 curve. The susceptibilities are too high in both cases. The Pd_4 curve is located above the $Pd_{31}Ag$ curve and exhibits a very pronounced maximum, which is considerably reduced for the supercell result. This

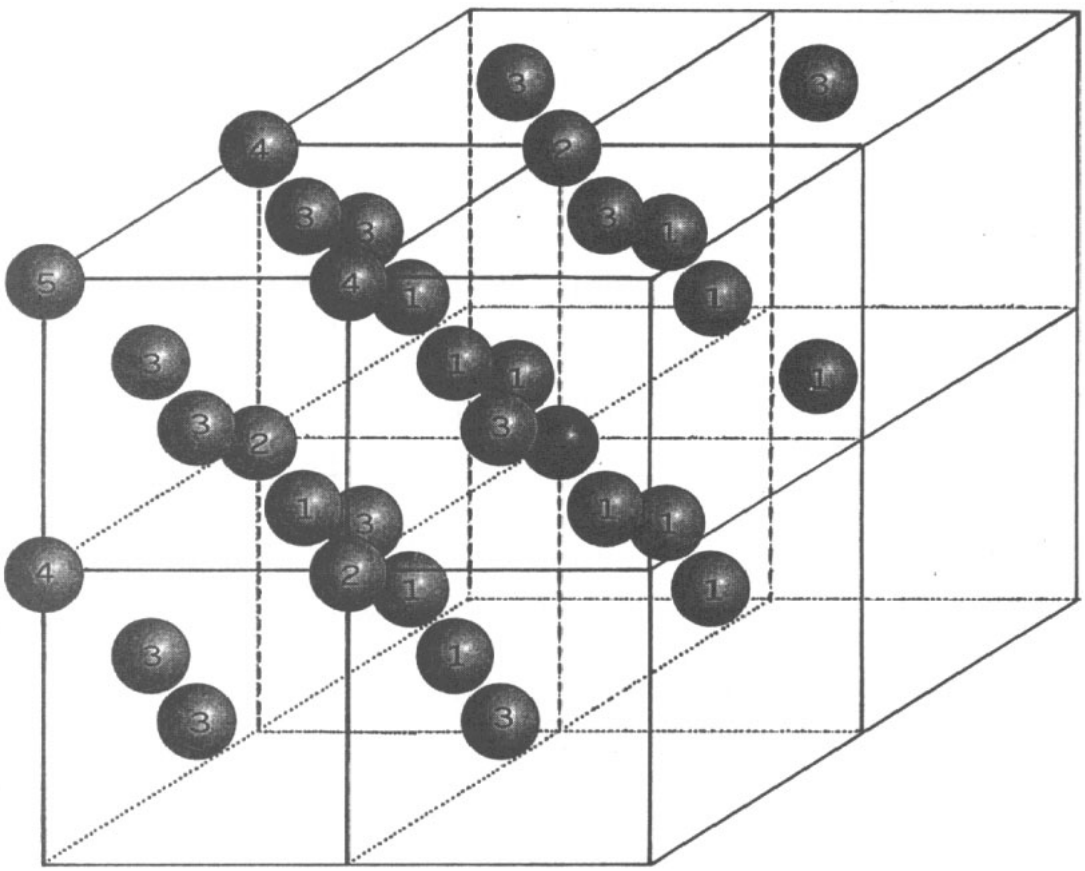

Figure 7. The supercell $Pd_{31}Ag$. The black ball represents the Ag atom. The numbers on the Pd atoms (hatched balls) indicate the shell to which they belong.

behaviour correlates with experiment.

Analogous results for the $Pd_{32}H$ system are collected in figure 9. The susceptibility of the theoretical curves is again too high compared with experiment, but the susceptibility curve for $Pd_{32}H$ is located correctly below the corresponding Pd_4 curve. Finally the maximum of the calculated alloy curve is shifted to lower temperature.

As mentioned in chapter 2 our method is very sensitive with respect to inaccuracies of the bandstructure results, which strongly influence the low-temperature regime. This might explain the low-temperature peaks of the curves, which do not correspond to experiment.

We would like to emphasize that the inconsistencies among the different curves (for example in figures 6, 8 and 9) are also observed in the corresponding $B'(M)$ curves and can therefore be ascribed to numerical instabilities of the bandstructure method. This effect is most obvious for the Pd_4 calculations shown in figures 8 and 9, whose input data differ in the lattice parameter by only 0.03‰. Apparently an accurate calculation of $B'(M)$ means a critical test for the bandstructure method.

Note also that changes in q_0 influence the scaling of the temperature axis via equation (2), but never alter the value of $\chi(\langle m^2\rangle)$ calculated with formula (1). On the other hand the relation between $\langle m^2\rangle$ and T is affected by the susceptibility for $T = 0$ (cf. equation (2)), which is a rather uncertain quantity, if it is calculated with our bandstructure program. Choosing an individual value for q_0 for each $\chi(T)$ curve, we compensate for this influence of $\chi(0)$ on the temperature axis to obtain the same decay for all curves at high temperatures. Crossings of different curves will then be avoided.

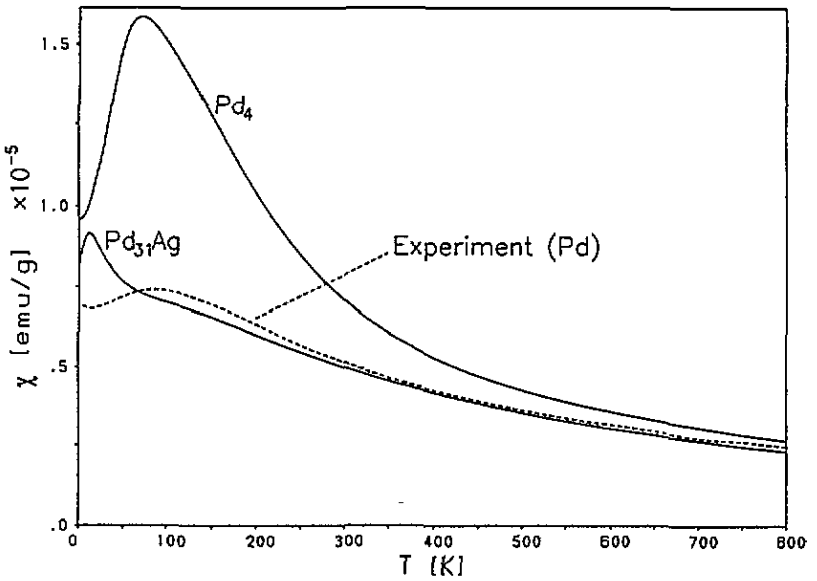

Figure 8. The susceptibility of $Pd_{31}Ag$ based on a non-relativistic ASW calculation for the lattice parameter 14.88 au and the corresponding result for Pd_4, $a = 7.44$ au. $q_0 = 0.038 \times 2\pi a^{-1}\ K^{-1/3}$.

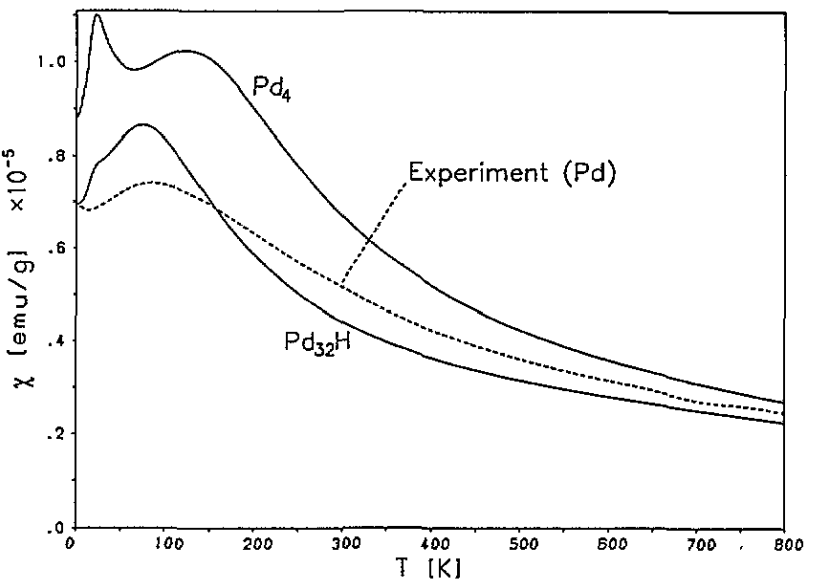

Figure 9. The susceptibility of $Pd_{32}H$ based on a non-relativistic ASW calculation for lattice parameter 14.876 au and the corresponding result for Pd_4, $a = 7.438$ au. $q_0 = 0.04, 0.038 \times 2\pi a^{-1}\ K^{-1/3}$.

In the supercell calculations equation (1) was evaluated with 44 mesh points each of which required a self-consistent calculation for a final field stability of 10^{-7} Ryd/μ_B.

In view of the enormous amount of computer time and the limited accuracy of the supercell calculations we chose another method to simulate low hydrogen concentrations in Pd with the ASW program. We increased the valence electron concentration of the primitive

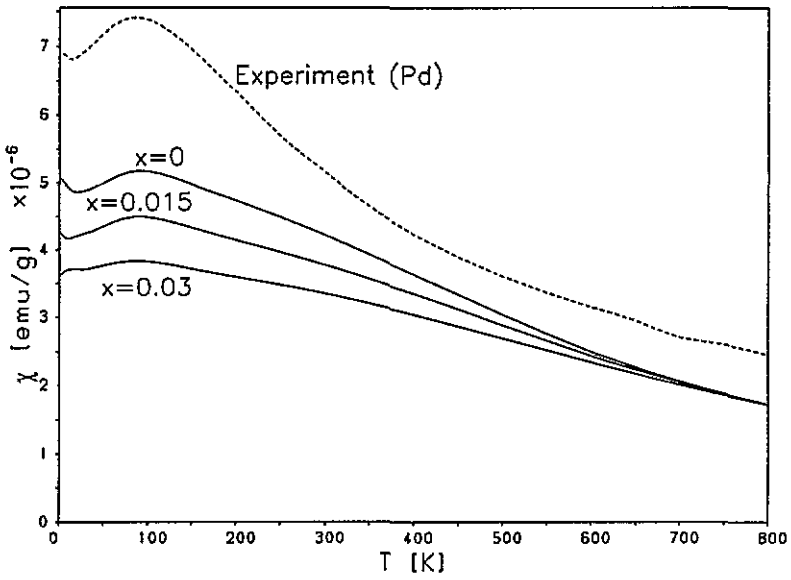

Figure 10. The susceptibility of PdH_x based on non-relativistic ASW calculations for a lattice parameter of 7.4 au. The low hydrogen concentration was simulated by additional valence charges (see the text). $q_0 = 0.06 \times 2\pi a^{-1}$ K$^{-1/3}$.

Pd cell by the impurity concentration thus taking into account the hydrogen electron, yet neglected the proton. In this way the contribution of the hydrogen electron to the valence charge may have been overestimated, since low-lying hydrogen states, which are neglected in this model, will partially pick up the hydrogen electron [22]. The results of this model for H concentrations of 1.5 and 3%, as well as the curve for pure Pd, with a lattice parameter of 7.4 au are shown in figure 10. Apart from the fact that the susceptibility of even pure Pd is too low, the results are in agreement with experiment with regard to the existence of a maximum. It has to be kept in mind that this procedure overestimates the hydrogen concentration as mentioned above.

4. KKR–CPA results

We also performed calculations with the KKR–CPA technique [13], which can be applied to non-stoichiometric random alloys. The KKR–CPA program supplied by Akai [14] was a scalar relativistic version for substitutional alloys.

Figure 11 shows susceptibility curves of $Pd_{1-x}Ag_x$ for $0 \leqslant x \leqslant 0.03$ and the theoretical equilibrium lattice parameter of 7.42 au. In agreement with experiment we obtain a maximum for the pure Pd curve, which disappears at 2% Ag. The susceptibilities continously decrease with increasing Ag concentration, yet are always higher than the experimental ones. Apart from the high susceptibilities and the overestimated influence of the Ag impurity the general features of the calculated curves agree with experiment.

Figure 12 shows the same calculations for the lattice parameter 7.35 au. The curves are similar to those in figure 11, the susceptibilities being in better agreement with experiment, but the maximum being less pronounced.

Calculations on pure Pd using a non-relativistic potential did not show a maximum. The maximum might thus be of relativistic origin, yet calculations on Pd with a scalar relativistic

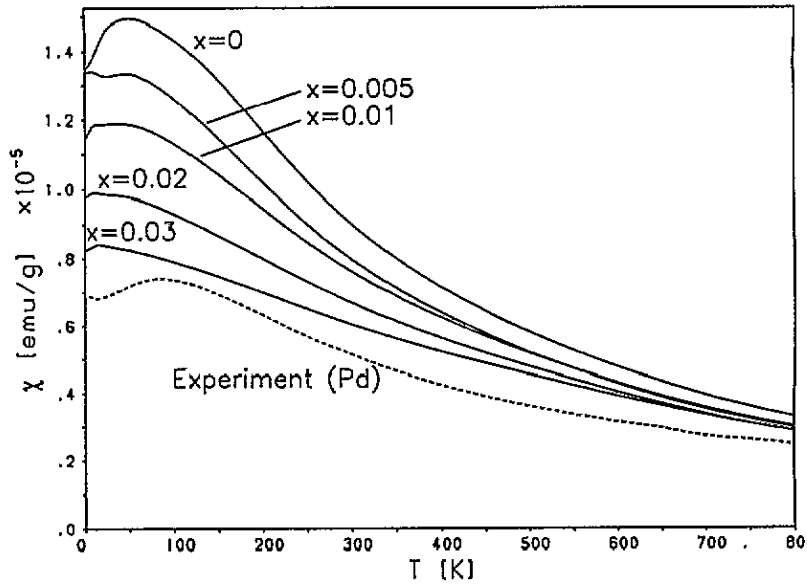

Figure 11. The susceptibility of $Pd_{1-x}Ag_x$ based on scalar relativistic KKR–CPA calculations for the lattice parameter 7.42 au and impurity concentrations 0, 0.5, 1, 2 and 3%. The corresponding values of q_0 are 0.04, 0.042, 0.042 and 0.043, $0.043 \times 2\pi a^{-1}$ $K^{-1/3}$.

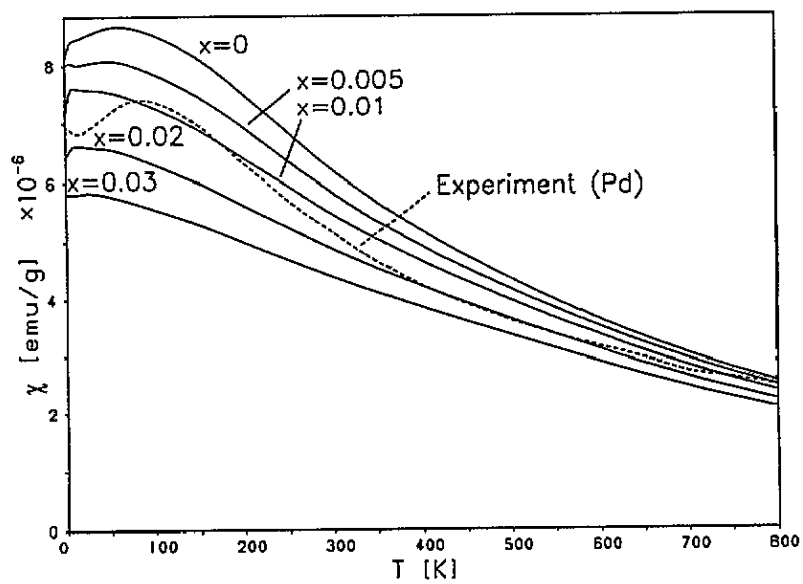

Figure 12. The susceptibility of $Pd_{1-x}Ag_x$ based on scalar relativistic KKR–CPA calculations for a lattice parameter 7.35 au and impurity concentrations 0, 0.5, 1, 2 and 3%. The corresponding values of q_0 are 0.05, 0.05, 0.052, 0.054 and $0.056 \times 2\pi a^{-1}$ $K^{-1/3}$.

ASW version likewise did not produce a maximum. This situation is unsatisfactory of course, because it means that a clear statement about the importance of relativistic effects cannot be made so far. We think that the use of a more sophisticated bandstructure method will be helpful with regard to this question.

5. Comparison with the Stoner theory

In order to derive the formulas (1)–(3) for the temperature-dependent susceptibility we applied spin fluctuation theory, which is based upon collective mode excitations. Today spin fluctuations are considered to be of decisive importance for the temperature behaviour of itinerant systems [23]. On the other hand the thermal excitations of Stoner's theory [24, 25] are particle–hole excitations with a spin flip not including collective phenomena. In this chapter we compare the susceptibility obtained from formulas (1)–(3) with that calculated in terms of the Stoner theory.

The formula for the inverse susceptibility of Stoner's theory is given by [26]

$$\chi^{-1}(T) = \left[-\mu_B^2 \int_{-\infty}^{\infty} N(\epsilon) f'(\epsilon)\, d\epsilon \right]^{-1} - \frac{I}{2{\mu_B}^2}. \tag{5}$$

$N(\epsilon)$ is the density of states for both spins, I the Stoner parameter and $f(\epsilon)$ the Fermi distribution function

$$f(\epsilon) = \left[1 + \exp\left(\frac{\epsilon - \mu}{k_B T} \right) \right]^{-1}.$$

Note that the chemical potential μ is determined implicitly by

$$\int_{-\infty}^{\infty} N(\epsilon) f(\epsilon)\, d\epsilon = n_e \tag{6}$$

(n_e is the number of electrons per unit cell), and therefore depends on the temperature.

In order to obtain the susceptibility for a given temperature the corresponding μ was calculated from equation (6), and subsequently $\chi^{-1}(T)$ from equation (5). The integration of f' in (5) with sufficient accuracy, in particular for low T, demands a very fine integration mesh around μ. In figure 13 we have plotted the susceptibility curves for Pd. The density of states was calculated with the tetrahedron method of ASW using 5900 tetrahedrons in the irreducible wedge of the first Brillouin zone. The Stoner parameter I was chosen for coincidence of the theoretical and experimental curves at $T = 0$. Again a maximum can be found, but, compared to the results of sections 3 and 4, the susceptibility curves extend to higher temperatures.

To compare these results with spin fluctuation theory the electron interaction had to be taken into account in a similar manner as in the Stoner theory. $B(M)$ was therefore calculated according to

$$B(M) = \frac{\epsilon_F^{\uparrow} - \epsilon_F^{\downarrow}}{2\mu_B} - \frac{IM}{2{\mu_B}^2} \tag{7}$$

in which the difference of the Fermi energies was obtained within the rigid-band model from a density of states for $M = 0$. Equation (7) is the expression for the external field in the Stoner theory, where the electron interaction is contained completely in the second term. Again I was adjusted to the experimental value at $T = 0$. The results for the same lattice parameters as in figure 13 are shown in figure 14. Similar to what is found for the curves presented in the previous two chapters, the maximum appears at about 80 K. As will be shown in the next section the different results of the spin fluctuation and Stoner theories are mainly due to a different influence of the electron interaction on the scaling of the temperature axis in the two theories.

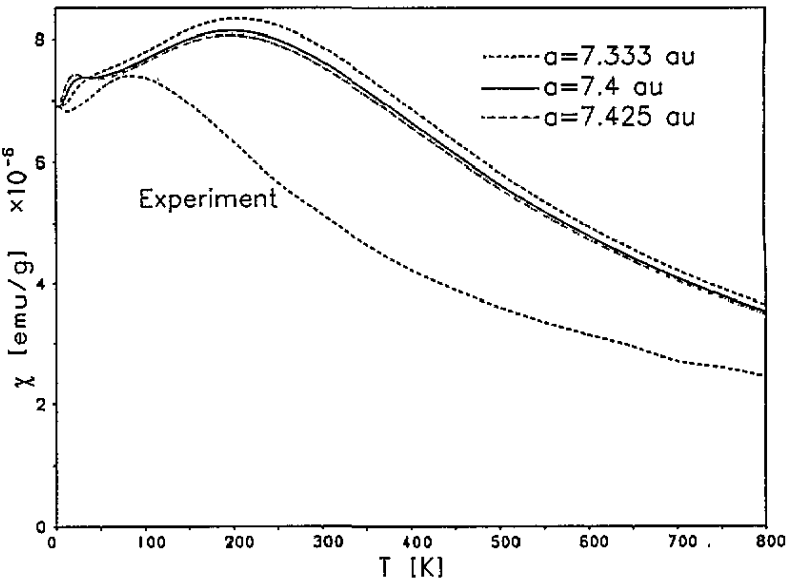

Figure 13. The susceptibility of Pd (Stoner theory) based on ASW calculations for lattice parameters 7.333, 7.40 and 7.425 au. The Stoner parameter was adjusted to the experimental value for $T = 0$.

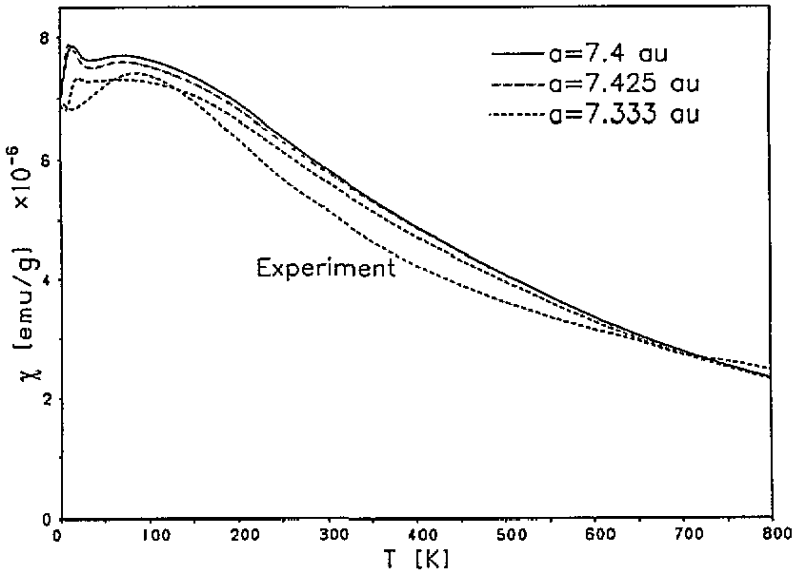

Figure 14. The susceptibility of Pd within the rigid-band model spin fluctuation theory (refer to the text), based on ASW calculations for lattice parameters 7.333, 7.40 and 7.425 au. $q_0 = 0.05 \times 2\pi a^{-1}$ K$^{-1/3}$. The Stoner parameter was adjusted to the experimental value for $T = 0$.

6. Discussion

As can be seen from equation (5), the parameter of the electron interaction I in Stoner theory causes a vertical shift of the inverse susceptibility, leaving the horizontal position of

the maximum in figure 13 unchanged.

On the other hand, in spin fluctuation theory there is a natural dependence of χ^{-1} on $\langle m^2 \rangle$ as demonstrated by equation (1). The relation between $\langle m^2 \rangle$ and T is determined by equation (2), which in turn involves the fluctuation-dependent inverse susceptibility. Since the electron interaction enters the susceptibility, it also affects the $\langle m^2 \rangle$ versus T curve, and thus the scaling of the susceptibility on the T axis. Thus the position of the maximum is affected by the strength of the electron interaction. For an estimate of this effect we neglect the wavevector dependence of χ^{-1} and write the susceptibility as

$$\chi(\langle m^2 \rangle) = S\chi^{\mathrm{P}}(\langle m^2 \rangle).$$

χ^{P} is the Pauli susceptibility and S the enhancement factor. From equation (2) we then obtain

$$\langle m^2 \rangle = \frac{k_{\mathrm{B}} T q_{\mathrm{c}}^3}{6\pi^2} S\chi^{\mathrm{P}}(\langle m^2 \rangle).$$

This leads to a scaling of the temperature axis as

$$T \sim \frac{\langle m^2 \rangle}{S} \tag{8}$$

for a constant cut-off wavevector q_{c}, and as

$$T \sim \left[\frac{\langle m^2 \rangle}{S}\right]^{1/2} \tag{9}$$

for $q_{\mathrm{c}} = q_0 T^{1/3}$, as used for all plots in this paper. With a typical enhancement factor $S = 9$ for Pd metal equation (9) predicts the susceptibility maximum of spin fluctuation theory at a temperature one third of that from the Stoner theory. This is in good agreement with figures 13 and 14.

A microscopic foundation for equation (8) can easily be given. In a recent paper [19] we showed that the excitation energies of the Stoner and spin fluctuation theories are comparable for non-interacting systems, leading to the same shape of the susceptibility curves. In the same paper an explicit formula for the partition function of an interacting system was derived,

$$Z = \int \frac{\mathrm{d}m_0}{\sqrt{2\pi}} \iint \left(\prod_{q_z > 0} \frac{1}{\pi} \, \mathrm{d}m_q \, \mathrm{d}m_{-q} \right) \exp(-\beta \mathcal{H}[m]) \tag{10}$$

where the quadratic term of the energy functional $\mathcal{H}[m]$ was given by

$$\frac{1}{2} \sum_q \chi^{-1}(q) |m_q|^2 . \tag{11}$$

With a constant cut-off wavevector q_{c} in equations (10) and (11) the enhancement factor S of $\chi(q)$ causes the curves to shrink on the temperature axis in agreement with equation (8).

Since the maximum of the Pd curves appears in both theories we suppose that its origin lies in the bandstructure. To investigate this point in greater detail we drew bandstructure plots from ASW calculations on Pd for a series of magnetizations. The bandstructure for $M = 0$ is shown in figure 15. Since the minority-spin bands are shifted to higher energies with increasing magnetization, the spin-down bands located approximately 3 mRyd below ϵ_{F} near the L point of the Brillouin zone and the Fermi level approach each other and converge at $M \approx 0.1 \mu_{\mathrm{B}}$. This effect leads to a slight increase of the density of states at the

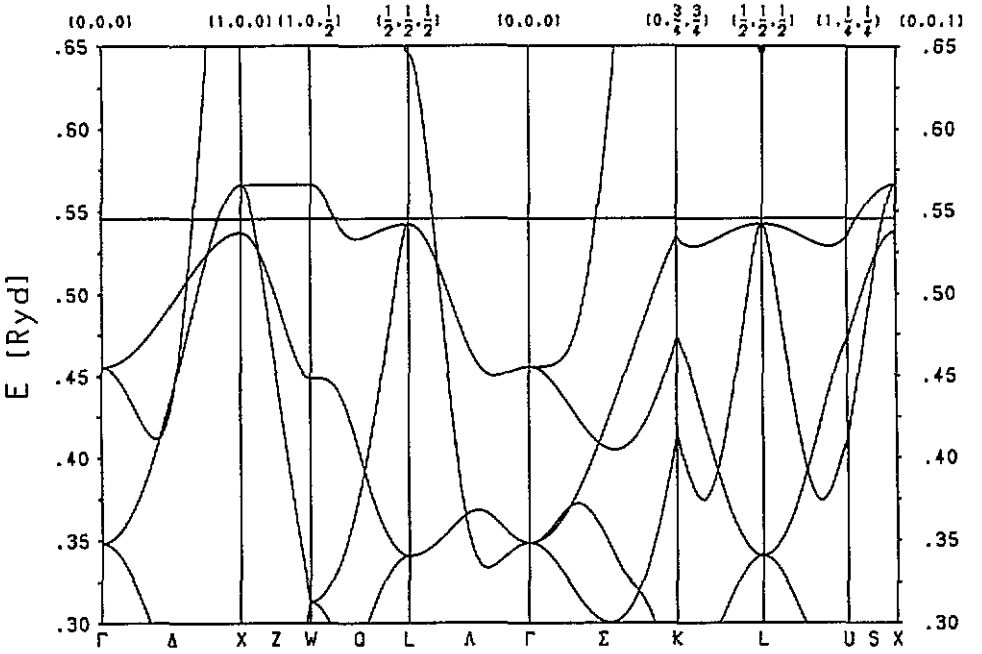

Figure 15. The bandstructure of Pd from an ASW calculation for the lattice parameter 7.425 au and zero magnetization.

Fermi energy of the spin-down band. Within the rigid band model the inverse susceptibility as a function of M is obtained by differentiation of equation (7), which gives

$$\chi^{-1}(M) = \frac{1}{4\mu_B^2}\left[\frac{1}{N(\epsilon_F^{\uparrow})} + \frac{1}{N(\epsilon_F^{\downarrow})}\right] - \frac{I}{2\mu_B{}^2}.$$

Thus the maximum in the density of states at $M \approx 0.1\mu_B$ causes a minimum in the $\chi^{-1}(M)$ curve, and thus a minimum of $\chi^{-1}(T)$ by virtue of equation (1).

In this context it should be mentioned that in both models, the Stoner theory as well as rigid-band-based spin fluctuation theory, the Stoner parameter I shifts the $\chi^{-1}(T)$ curve to lower values as can be seen from equation (5) and equations (7) and (1). By this mechanism the electron interaction magnifies all structures present in the non-interacting susceptibility $\chi^P(T)$ and thus enhances the maximum by a factor of S. In other words the maximum of the curves in figures 13 and 14 is hardly observable for $I = 0$.

The susceptibility curves from the calculations presented in sections 3 and 4 are less easy to understand, because the electron interaction is not treated with a single parameter, but with a self-consistently determined potential. Nevertheless, we suppose that the same mechanism holds as pointed out above; that is, the maximum is due to bands approaching the Fermi surface near the L point and is enhanced by a factor of S through interaction effects.

7. Summary

We applied our recently presented method to the calculation of the temperature-dependent magnetic susceptibility of Pd and the alloys $Pd_{1-x}Ag_x$ and PdH_x obtaining the input data from ASW and KKR–CPA bandstructure calculations. The non-relativistic ASW calculations

and the scalar relativistic KKR–CPA calculations for Pd yield a maximum of $\chi(T)$ near the experimental value of 80 K. The ASW curves lie below, the KKR–CPA curves above the experimental ones.

In order to simulate the alloys for $x = 0.03$ the ASW program was applied to the supercells $Pd_{31}Ag$ and $Pd_{32}H$. The supercell results yield susceptibility values too high compared with experiment. However, in relation to the corresponding Pd_4 calculations, where the same k-vectors for the Brillouin zone integration were used, they reflect the experimental trend.

As an alternative to the ASW supercell calculations we simulated low hydrogen concentrations in PdH_x by calculations for pure Pd with increased valence electron concentration. The susceptibility turns out to be too low, yet the general features of the curves agree with experiment.

The decay of the susceptibility maximum of the $Pd_{1-x}Ag_x$ alloys with increasing Ag concentration could be reproduced satisfactorily with KKR–CPA calculations.

A detailed comparison of $\chi(T)$ of Pd from the Stoner theory and from spin fluctuation theory with rigid bands indicated that the temperature axis is scaled by the factor $S^{-1/2}$ in spin fluctuation theory. Furthermore, the maximum of $\chi(T)$ of Pd could be explained by the shape of the bandstructure at the L point of the Brillouin zone and its modification with finite magnetization.

Acknowledgments

We are grateful to Professor K Schwarz and Dr P Mohn, TU Wien, for supplying the ASW bandstructure program, and to Professor J Kübler, TH Darmstadt, for providing a scalar relativistic extension to it. We would also like to thank Professor H Akai, NARA Medical University, and Professor H Ebert, Universität München, for supplying and installing the KKR–CPA program. Professor P C Schmidt, TH Darmstadt, inspired the simulation of the PdH_x alloy (figure 10).

References

[1] Manuel A J and St Quinton J M P 1963 *Proc. R. Soc.* A **273** 412
[2] Weiss W D and Kohlhaas R 1967 Z. *Angew. Phys.* **23** 175
[3] Hahn A and Treutmann W 1969 Z. *Angew. Phys.* **26** 129
[4] Jamieson H C and Manchester F D 1972 *J. Phys. F: Met. Phys.* **2** 323
[5] Shimizu M, Takahashi T and Katsuki A 1963 *J. Phys. Soc. Japan* **18** 240
[6] Liu K L, MacDonald A H, Daams J M, Vosko S H and Koelling D D 1979 *J. Magn. Magn. Mater.* **12** 43
[7] Vosko S H and Perdew J P 1975 *Can. J. Phys.* **53** 1385
[8] Irkhin Yu P and Rosenfeld E W 1982 *Solid State Commun.* **44** 1371
[9] Mohn P and Schwarz K 1992 *J. Magn. Magn. Mater.* **104–107** 685
[10] Murata K K and Doniach S 1972 *Phys. Rev. Lett.* **29** 285
[11] Kirchner B, Weber W and Voitländer J 1992 *J. Phys.: Condens. Matter* **4** 8097
[12] Williams A R, Kübler J and Gelatt C D 1979 *Phys. Rev.* B **19** 6094
[13] Faulkner J S 1982 *The Modern Theory of Alloys (Progress in Materials Science 27)* (Oxford: Pergamon)
[14] Akai H 1989 *J. Phys.: Condens. Matter* **1** 8045
[15] Treutmann W 1968 *PhD Thesis* Marburg
[16] Wagner D 1989 *J. Phys.: Condens. Matter* **1** 4635
[17] Murata K K 1975 *Phys. Rev.* B **12** 282
[18] Lonzarich G G and Taillefer L 1985 *J. Phys. C: Solid State Phys.* **18** 4339
[19] Weber W, Kirchner B and Voitländer J 1994 *Phys. Rev.* B submitted
[20] Williams A R, Moruzzi V L, Kübler J and Schwarz K 1984 *Bull. Am. Phys. Soc.* **29** 278
[21] Stenzel E and Winter H 1986 *J. Phys. F: Met. Phys.* **16** 1789

[22] Switendick A C 1978 *Hydrogen in Metals I (Topics in Applied Physics 28)* ed G Alefeld and J Völkl (Berlin: Springer) p 101
[23] Moriya T 1985 *Spin fluctuations in Itinerant Electron Magnetism (Springer Series in Solid-State Sciences 56)* (Berlin. Springer)
[24] Stoner E C 1936 *Proc. R. Soc.* A **154** 656
[25] Stoner E C 1938 *Proc. R. Soc.* A **165** 372
[26] Gautier F 1982 *Magnetism of Metals and Alloys* ed M Cyrot (Amsterdam: North-Holland) p 10